We are IntechOpen, the world's leading publisher of Open Access books
Built by scientists, for scientists

6,900
Open access books available

186,000
International authors and editors

200M
Downloads

154
Countries delivered to

Our authors are among the

TOP 1%
most cited scientists

12.2%
Contributors from top 500 universities

CLARIVATE ANALYTICS
BOOK CITATION INDEX
INDEXED

WEB OF SCIENCE™

Selection of our books indexed in the Book Citation Index
in Web of Science™ Core Collection (BKCI)

Interested in publishing with us?
Contact book.department@intechopen.com

Numbers displayed above are based on latest data collected.
For more information visit www.intechopen.com

Nanostructured Morphologies by Self-Assembly of Diblock Copolymers: A Review

Galder Kortaberria

Additional information is available at the end of the chapter

Abstract

Due to the thermodynamic incompatibility between blocks, diblock copolymers can self-assemble in a wide variety of nanostructures, covalent linkage among blocks preventing the phase separation at macroscopic scale. Those nanostructures depend on copolymer composition (f), Flory-Huggins interaction parameter among both blocks (χ), and polymerization degree of the copolymer (N). Thin films of block copolymers can show different equilibrium morphologies such as spheres, cylinders, gyroids, and lamellas. Besides mentioned parameters, film preparation process (substrate, annealing process if any) and used solvent will determine self-assembled morphology. In the present review, the most important morphologies or microstructures obtained for different diblock copolymer films are presented, as well as the most important phase transitions among them. Different microstructures and the way in which they can be obtained become of great importance, as they could be used as templates for nanoparticle deposition, nanolithography, or nanopatterned materials with several potential applications in different fields such as nanoelectronics or nanomedicine.

Keywords: self-assembly, nanostructure, morphology, lamellar, cylinders, gyroids

1. Introduction

Block copolymers consist in macromolecules produced by joining two or more chemically distinct polymer blocks, that may be thermodynamically incompatible. Segregation of these blocks on the molecular scale (5–100 nm) can produce many different complex nanostructures. More than three decades of theoretical development have culminated in remarkably predictive statistical theories that can account for the domain shapes, dimensions, connectivity and ordered symmetry of many types of block copolymers. Nowadays, the possibility to

join blocks in novel molecular architectures can produce a really huge number of structured materials endowed with tailored mechanical, optical, electrical, barrier, and other physical properties [1, 2].

Many different block configurations can be constructed with different synthetic chemistry techniques. Based on the number of chemically distinct blocks, and their linear or branched sequencing linear and branched diblock copolymers, linear ABC triblock copolymers and ABC star or heteroarm triblock copolymers can be distinguished. Those would be the most important ones, even if block copolymers with more than three blocks can be also found.

The simplest and most studied architecture is the linear AB diblock, consisting of a long sequence of A type monomers covalently bonded to a chain of B type monomers. $(AB)_n$ multiblocks are formed by coupling additional A and B blocks. Morphologies obtained by self-assembly of diblock copolymers in films will be shown and reviewed in the present chapter.

Due to the thermodynamic incompatibility between blocks and the covalent bond among them that avoids macrophase separation, block copolymers can result in many different nanostructures [1, 3, 4]. For this reason, many researchers have shown interest in block copolymers during the last decade [5–7]. Block copolymers can self-assemble into different nanostructures that depend on several parameters such as copolymer composition (f), Flory-Huggins interaction parameter among both blocks (χ), and polymerization degree of the copolymer (N). Spheres, cylinders, gyroids, and lamellas are the usual equilibrium nanostructures shown by diblock copolymers either in bulk or in thin films [8–11] as it can be seen in **Figure 1**.

N and f, related to the translational and conformational entropy of the copolymer, respectively, can be tuned by polymerization reaction, while χ reflects enthalpic interactions among blocks. As a result, χN represents the enthalpy related to the linkage of two different polymer chains. In thin films of block copolymers, the orientation and lateral ordering of the microdomains are influenced by factors like χN, interfacial interactions at the air/polymer and polymer/substrate interfaces, and the commensurability between the equilibrium period (L_o) and film thickness [12, 13]. A parallel orientation of the cylindrical and lamellar microdomains is observed when there is a large difference in the surface energies of the two blocks and/or a strong preferential interaction of one block with the substrate. However, sometimes it is desirable to be able to orient the microdomains normal to the film surface. As the molar mass of the copolymer mainly determines the size of micro or nanodomains, it can be quite easily controlled by the polymerization process.

In the present chapter, a deep review on the generation of nanostructures by self-assembly of diblock copolymers in thin films is presented. Besides classical lamellar, cylindrical or spherical morphologies obtained for many different diblock copolymers, more complex nanostructures such as perforated lamellae or bicontinuous gyroids will be shown as obtained by several authors for many different diblock copolymer types.
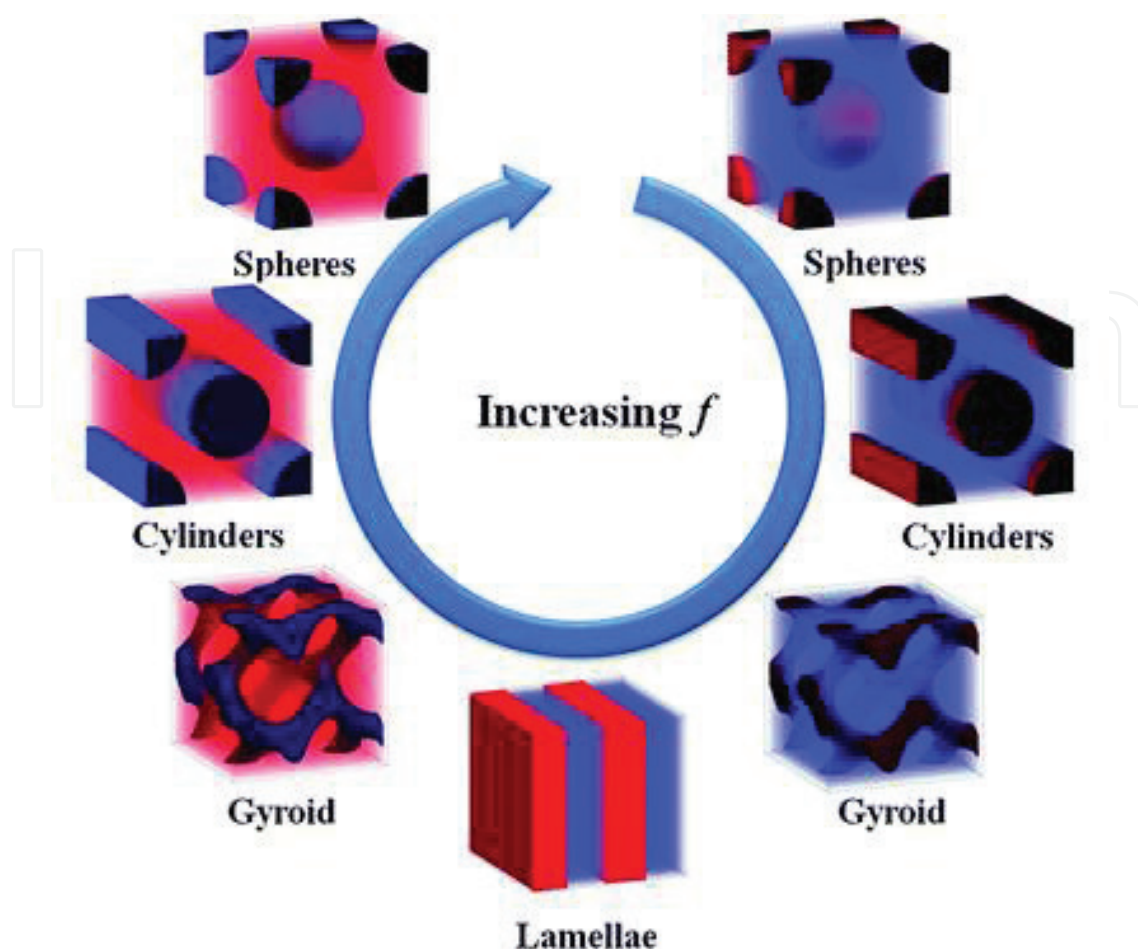
Figure 1. Various nanostructures formed by the self-assembly of block copolymers. The *f* indicates the volume fraction of one component. Reproduced with permission of Soft Matter 2013, 9, 9059. Copyright 2013, Royal Society of Chemistry.

2. Morphology of diblock copolymer thin films

Matsen and Schick [14] calculated the phase diagram for AB diblock copolymers. For $X_{AB}N < 10.5$, only a disordered melt is predicted. At larger values of $X_{AB}N$, above the order-disorder transition curve, five ordered microphase structures are predicted to have regions of thermodynamic stability. The lamellar (L) phase is stable for nearly symmetric diblocks, while a hexagonally packed cylinder (HPC) phase is stable for diblocks with intermediate levels of compositional asymmetry. With still more compositional asymmetry, the hexagonal phase gives way to a body-centered cubic spherical (BCC-sphere) phase. A very narrow region of close-packed spheres (CPS) separates the disordered and sphere phases at the composition extremes. Finally, Matsen and Schick predicted narrow regions of stability of a complex gyroid (G) phase close to the order-disorder transition and between the L and HPC phases. All those morphologies obtained for different block copolymers will be shown together with some others like perforated lamellae.

2.1. Lamellar morphology

It constitutes the stable phase for symmetric diblock copolymers. It has been commonly found for many diblock copolymer thin films, both without any further treatment or after thermal or solvent vapor annealing. Both thermal and solvent annealing methods have been used to bring the samples into their equilibrium states and to reduce the number of defects [15]. Lamellar morphology can be used to create line and space patterns on substrates by controlling their orientation. Lamellar orientation depends on several parameters and/or factors such as the substrate used for film preparation [16, 17], thermal or solvent vapor annealing treatments [15, 17, 18], chain length or molar mass [16, 17, 19], pressure application during annealing [20] or the use of graphoepitaxial techniques for film preparation [21–23]. Thus, different orientations have been obtained for different block copolymers by controlling those parameters.

Regarding the effect of substrate used for preparing the films, different orientations of lamellar microdomains have been found for poly(styrene-*b*-methyl methacrylate) (PS-*b*-PMMA) diblock copolymer by using random PS-r-PMMA copolymer-grafted substrates [16]. The control of styrene fraction in random copolymers allowed tuning the interfacial interactions at the substrates from PS-selective to PMMA-selective. Parallel orientations of lamellar microdomains were found for all substrates except in the case of a neutral substrate, for which no lamellar structure was obtained, attributed to surface compatibility between PS and PMMA blocks at the substrate. The importance of substrate on lamellar orientation and structure also has been seen for poly(ethylene oxide-*b*-buthylene oxide) (PEO-*b*-PBO) copolymer by preparing films both in mica and silicon substrates [17]. For films annealed under vacuum, a half-layered, densely branched structure was found for films prepared on mica. For films prepared on silicon, however, a half-layered structure without any meaningful feature was obtained. Probably, in the annealing treatment, the polymer chains located at the upper layers moved to the bottom ones. This makes the upper layers to progressively disappear. The thickness of the upper polymer layers became larger while that of the bottom layers in contact with mica decreased. An increase of lamellar thickness seemed to be the cause of both phenomena. In the first half layer, the increase of lamellar thickness led to spreading and half-layer thinning. In the upper layer, on the contrary, the islands contacted but got thicker. The interaction of PEO block with the substrate seemed to be reason for obtaining such a branched structure and differently oriented PEO crystals in the polymer layer in contact with mica. The effect of annealing process was also clearly seen, since as-cast films exhibited a multilayered structure with lamellar microdomains parallel to the surface for shorter copolymers, while for longer ones, the lamellar microdomains in the upper polymer layers exhibited mixed orientations of parallel and perpendicular lamellae.

Both thermal and solvent vapor annealing have also been used for the generation of lamellar morphologies with different orientations. In this way, the lamellar orientation of poly(styrene-*b*-butadiene) (PS-*b*-PB) copolymer has been found to be strongly dependent on solvent annealing process [15]. The reorientation of lamellae occurred during solvent vapor annealing with ethyl acetate. Films presented initially a distribution of lamellar orientations and the lamellar spacing depended on their orientation. Whereas the parallel lamellae presented the smallest

spacing, the perpendicular ones had the largest one. Due to the effect of substrate that constrained perpendicular lamellae, their swelling was more difficult than that of the parallel ones. However, the measured lamellar spacing was equal for both after a certain time of swelling. The swelling process changed the orientation of the lamellae they appearing completely parallel at the end of the process. Schematic evolution of structures during solvent vapor annealing process can be seen in **Figure 2**.

Thermal annealing also affects the formation and orientation of lamellar domains. For poly (styrene-*b*-caprolactone) (PS-*b*-PCL) copolymer [18] annealed at temperatures higher than T_g of both blocks, worm-like or lamellar morphologies with lamellae parallel to the surface were obtained at 100 and 120°C, respectively, as it can be seen in **Figure 3**. Moreover, the addition of magnetic nanoparticles modified with polymeric brushes in order to increase compatibility with matrix did not change obtained morphologies or lamellar orientations.

To perform the annealing process under vacuum constitutes another way to control the formation and orientation of lamellar microdomains [17, 20]. Highly oriented films can be obtained by annealing copolymer films under pressure. In this way, for a lamella-forming poly(styrene-*b*-ethylene oxide) (PS-*b*-PEO) annealed under a pressure of 0.2 MPa, a highly oriented structure has been obtained by the combined effects of shear flow and self-organization of the block copolymer during annealing under stress [20]. Annealing at high temperature under pressure was carried out in two steps: the melt-flow of the copolymer in the X–Y plane under pressure and the ordering of the lamellar structure during annealing at high temperature. The degree of orientation increased with annealing time.

Chain length and molar mass of copolymers also are key factors in order to obtain lamellar structures with different orientations [16, 17, 19]. For films of PS-*b*-PMMA prepared in a neutral substrate [16], it was found that the orientation of lamellar microdomains was strongly influenced by the molecular weight of the copolymer and film thickness. For the copolymer with low molar molecular weight (29,000 g/mol), a parallel orientation of lamellar microdomains was obtained over the film. When the molecular weight was increased to 113,000 g/mol, a greater number of perpendicularly oriented lamellae were seen close to the polymer/substrate interface. By a theoretical approach, authors demonstrated that lamellar orientation on a neutral substrate is mainly determined by the entropic contribution to the free energy. For copolymers with higher N values, the chain stretching (nematic effect) entropically favored
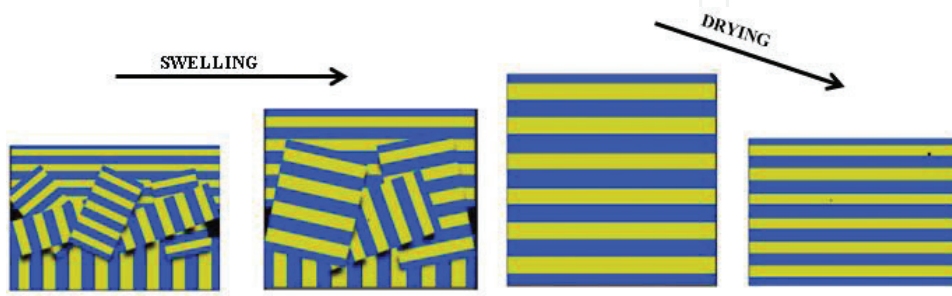

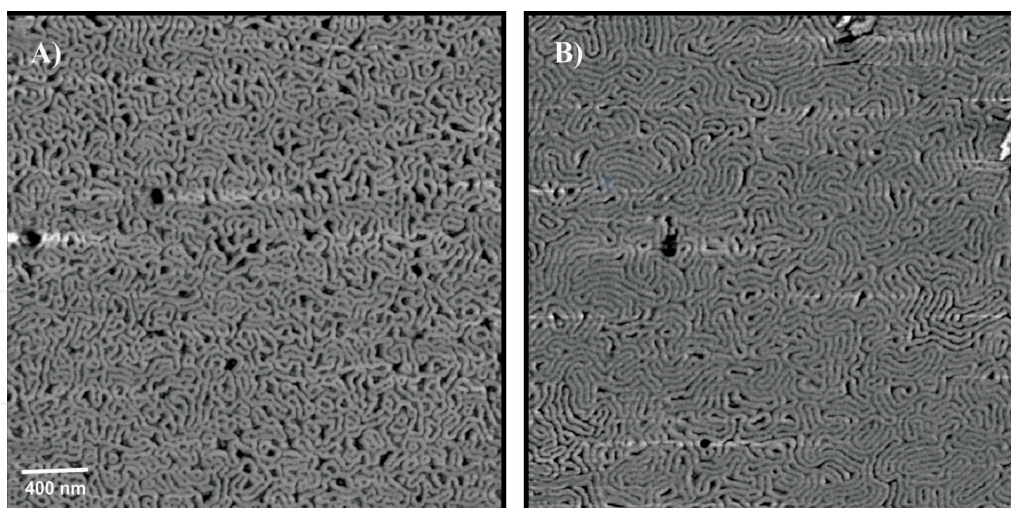**Figure 2.** Schematic structures of the thin film during swelling and drying.

Figure 3. AFM phase images of PS-*b*-PCL block copolymer annealed for 72 h at: (A) 100°C and (B) 120°C. Reproduced with permission of [18]. Copyright 2014, Elsevier.

the perpendicular orientation of lamellae, while for copolymers with lower N values, the chain-end effect dominated and the parallel orientation of lamellae was favored. The effect of molecular weight on lamellar orientation was also found for PEO-*b*-PBO copolymer thin films prepared on mica [17]. For shorter copolymers, a multilayered lamellar structure parallel to the surface was found. In the half layer in contact with the surface, the stems of PEO crystals were parallel to it, while they appeared perpendicularly oriented in the upper half layer. In the other hand, the as-cast thin film of copolymers with higher molecular weights showed a mixture of parallely and perpendicularly oriented lamellae. The effect of chain length has also been studied for PS-*b*-PB copolymer thin films, together with that of film thickness [19], varying film thickness/lamellar thickness ratios from 0.5 to 10. For ratios between 1 and 10, lamellae paralelly oriented to the surface were obtained for low molar masses (below 55 kg/mol), while perpendicularly oriented lamellae were obtained for copolymers with higher molar masses (above 90 kg/mol). On the other hand, for film thicknesses equal to the lamellar thickness, the films did not exhibit any texture, whereas for film thicknesses equal to the half of lamellar thickness, a weak surface structure could be observed. Authors claimed that it was consistent with symmetric wetting (the same block adsorbs at both film interfaces), but with weak selectivity. For blocks that interact only weakly with the substrate surface and with air, molar mass was seen to be the key factor for the lamellar orientation. Authors gave an explanation of their findings based on the theoretical model by Pickett et al. [24]. High molar masses favored the perpendicular lamellar orientation, while lower ones resulted in less ordered parallel lamellae, due to the different scaling behavior of entropic and enthalpic contributions to the interfacial energies with chain length. By studying the effect of molar mass on lamellar structures, in poly(cyclohexylethylene-*b*-methyl methacrylate) (PCHE-*b*-PMMA) thin films, some of the smallest lamellae observed were found [25]. Ordered lamellar domain pitches were identified by small-angle X-ray scattering for copolymers containing 43–52 vol% of PCHE block. Atomic force microscopy was used to show around 7.5 nm lamellar features, some of the smallest observed. For the lower molar mass sample, sub-5 nm nanodomains

were found, which together with the sacrificial properties of PMMA and the high overall thermal stability placed this material at the forefront of "high-χ" systems for advanced nanopatterning applications. Lamellae were found to be aligned perpendicularly to the surface.

Block copolymers have attracted considerable attention as fabrication method for nanopatterning, in which nanometer-sized domains are used as lithography templates. For dense line pattern formation, lateral lamellar domains are more preferable because in their case, an aspect ratio at least greater than 2 can be obtained. Epitaxial self-assembly by chemically or topographically nanopatterned substrates or resist patterns as guide have been demonstrated to be effective for lateral lamellar orientation [21–23]. In this way, lamellar domains of PS-*b*-PMMA symmetric copolymer have been successfully aligned on chemically nanopatterned substrates [23]. Advanced lithography allowed the induction of epitaxial self-assembly of domains in films. In this way, oriented patterns without defects were created over large areas. Obtained structures depend on the size and quality of the surface pattern rather than on the self-assembly process. **Figure 4** shows the two-step process used for the preparation of nanopatterned surfaces.

The lamellar microdomains of PS-*b*-PMMA followed the lithographically predefined surface patterns of chemical contrast. Bent block copolymer lamellae could be therefore obtained. Topographic guiding patterns have also been [21] used for bending lamellar microdomains, designed as elbows with varying corner angles. By controlling the surface of guiding patterns nonselective to the microdomains, the orientation of lamellae was rendered perpendicular to the surfaces of bottom and sidewalls of the guiding patterns. For both PS-*b*-PMMA and PS-*b*-PEO copolymers, authors demonstrated that bending of lamellar microdomains in block copolymer films could be formed within angled corners of topographic guiding patterns that exhibited a nonselective wetting property. Both lamellar-forming copolymers revealed similar bending trends. **Figure 5** shows the scheme of the procedure used to direct the self-assembly of block copolymers on topographic guiding patterns. Finally, also resist patterns have been used as guide for lamellar orientation [22]. In this way, the lateral alignment of symmetric PS-*b*-PMMA was achieved in confined spaces between straight guide patterns composed of a hydrogen silsesquioxane resist. It is worth to note that a lamellar structure with a period lower than that the pitch of the guide pattern was formed by this approach, while by chemically nanopatterned substrates, only structures with higher periods than the pitch of the guide pattern could be oriented.
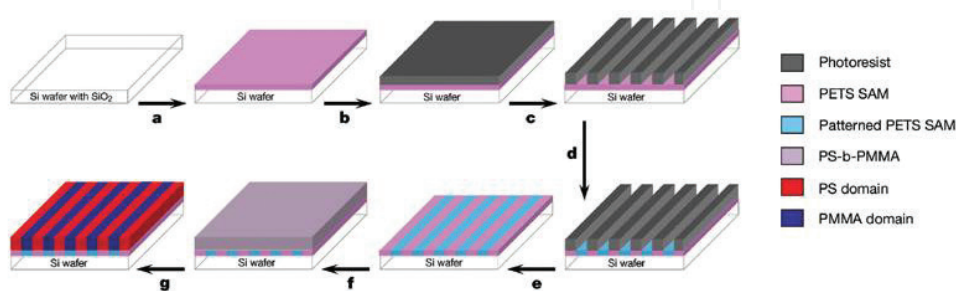

Figure 4. Two-step process for the preparation of nanopatterned surfaces for lamellar orientation of PS-*b*-PMMA copolymer. Reproduced with permission of [23]. Copyright 2003, Springer Nature.
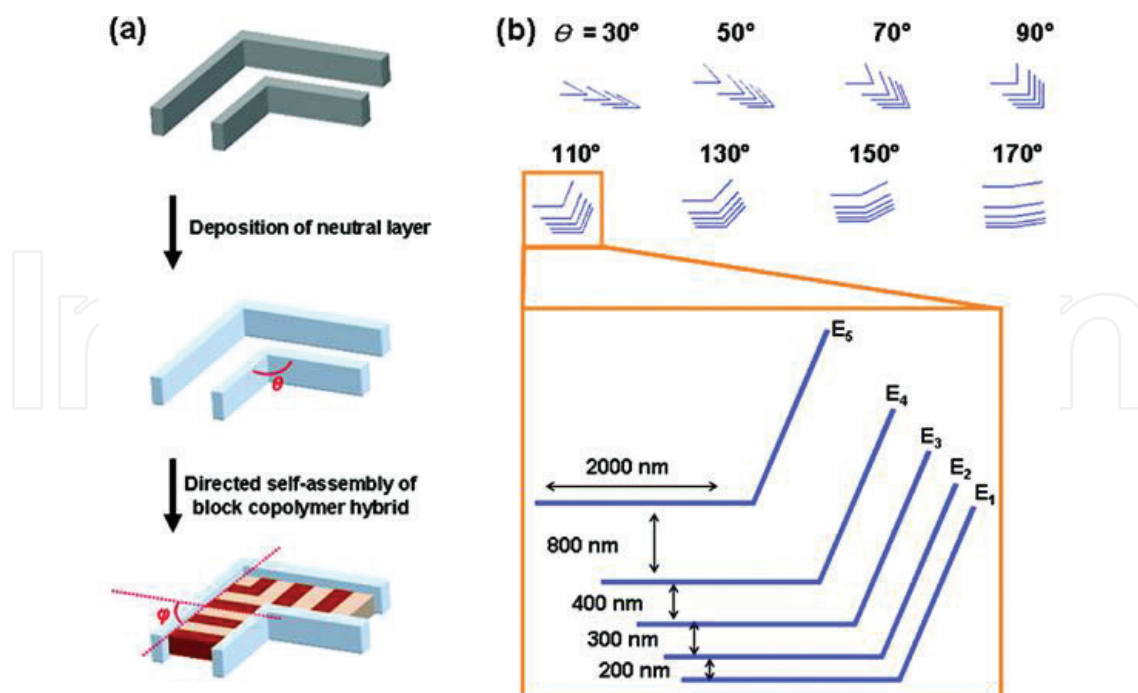
Figure 5. Schematic of the process used to direct the assembly of lamellae-forming block copolymers on topographic guiding patterns with bending geometries. (a) The procedure begins with the deposition of neutral layer followed by directed self-assembly of block copolymer thin films. (b) Diagram of topographic guiding patterns. Reproduced with permission of [31]. Copyright 2010, American Chemical Society.

2.2. Perforated lamellar morphology

Even if in the bulk state, the perforated lamellar morphology of block copolymers has been reported to be a metastable state of the gyroid (G) phase, under thin film confinement conditions, one-dimensional confinement provides stability to the phase [26, 27] and has been found for different diblock copolymer thin films under several conditions [26–35]. For thin films of poly(styrene-*b*-dimethylsiloxane) (PS-*b*-PDMS) diblock copolymer spin coated onto silicon wafers modified with hydroxyl-terminated PDMS subject to solvent vapor annealing, depending on the film thickness, its commensurability with the microdomain period, and the ratio of toluene/heptane vapors used for the solvent annealing process, perforated lamellae morphology can be obtained [26], besides spheres, cylinders, or gyroids. Even if PS-*b*-PDMS presented a double-gyroid morphology in bulk, as a thin film the morphology can be tuned by playing with different parameters. The solvent composition and pressure affected the relative Swelling of blocks, and therefore, the effective volume fraction, the swelled film thickness, and the effective χ. In-plane cylinders, HPL, and spheres with excellent long-range order and low defect levels were obtained at specific film thickness and solvent vapor compositions. For the same annealing conditions with 3:1 toluene/heptane ratio, hexagonally perforated lamellae (HPL) appeared and dominated as the film became thinner, as it can be seen in **Figure 6**.

At around 80 nm thickness, two layers of interconnected HPL were formed. Other solvent ratios produced mixed morphology structures such as comb-like patterns from coexisting
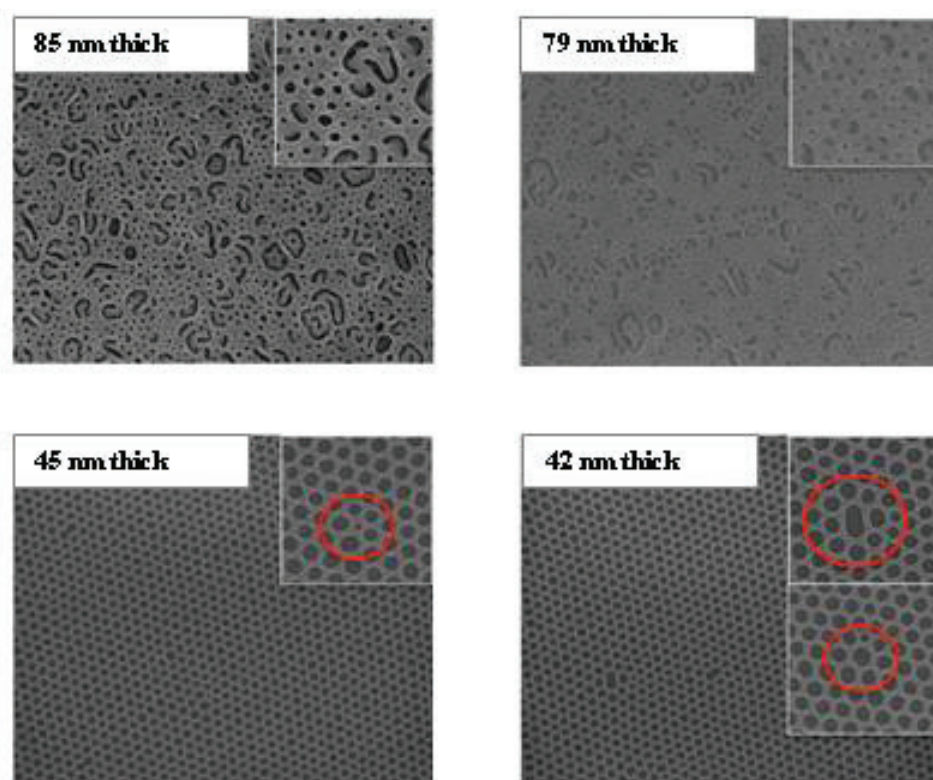
Figure 6. Representative SEM images of PDMS microdomains formed in thin films with differing initial thickness at the same solvent vapor annealing conditions. Reproduced with permission of [26]. Copyright 2014, American Chemical Society.

lamellae and cylinders. For thin film composites based on PS-*b*-PDMS copolymer with a volume fraction of 38% for PDMS and PS-modified Au nanoparticles (subjected to a thermally assisted solvent vapor treatment), an unique one-to-one positioning phenomenon of guest Au nanoparticles in the host microdomains was found; each of PS-functionalized nanoparticle appeared embedded within the perforation domain of HPL morphology of PS-*b*-PDMS. By controlling the weight fraction of Au-NPs and the effective volume fraction of constituent polymer blocks, individual nanoparticles were selectively incorporated into the centers of PS perforations of HPL morphology. The local minimization of free energy achieved by the placement of nanoparticles into the center of the perforation domain was theoretically supported by the self-consistent field theory (SCFT) simulation.

For poly(methyl methacrylate-*b*-vinyl-mtriphenylamine) (PMMA-*b*-PVmTPA) copolymers synthesized by RAFT polymerization with different PVmTPA fractions from 0.25 to 0.33, a variety of well-defined nanostructures were obtained [29]: HPC for a fraction of 0.27 and below, lamellae for fractions of 0.30 and above and HPL at an intermediate fraction of 0.29. The possibility of tuning morphologies obtaining different nanostructures for those block copolymers containing electro-active hole-transport components such as triphenylamine-based ones constitutes an attractive option for organic electronic applications in which well-defined nanoscale structures are desirable.

At a composition of 35 vol% of poly(methyl acrilate) (PMA), the formation of a HPL morphology was observed for a polydisperse poly(styrene-*b*-methyl acrilate) (PS-*b*-PMA) copolymer for short- and long-term solvent-casting conditions [30], as it can be seen in **Figure 7**. The hexagonal arrangement of the PS perforations is clearly visible in the upper right inset of the Figure which depicts a plane view of the PMA layer. The relative positions of the perforations furthermore indicated the ABC stacking of the PMA layers, characteristic for the rhombohedral structure. No order-order transitions were observed at elevated temperatures or after prolonged thermal annealing. The observed stabilization of the HPL morphology, considered to be metastable in narrow-disperse diblock copolymers as well as diblock copolymers with selective block polydispersity, suggested that the skewness of the distribution of block molecular weights is an important parameter for the structure selection during microphase separation. In particular, authors found that symmetric block molecular weight distributions made possible the stabilization of microstructures presenting higher standard deviation of mean curvature. Authors showed the importance of controlling the width and symmetry of
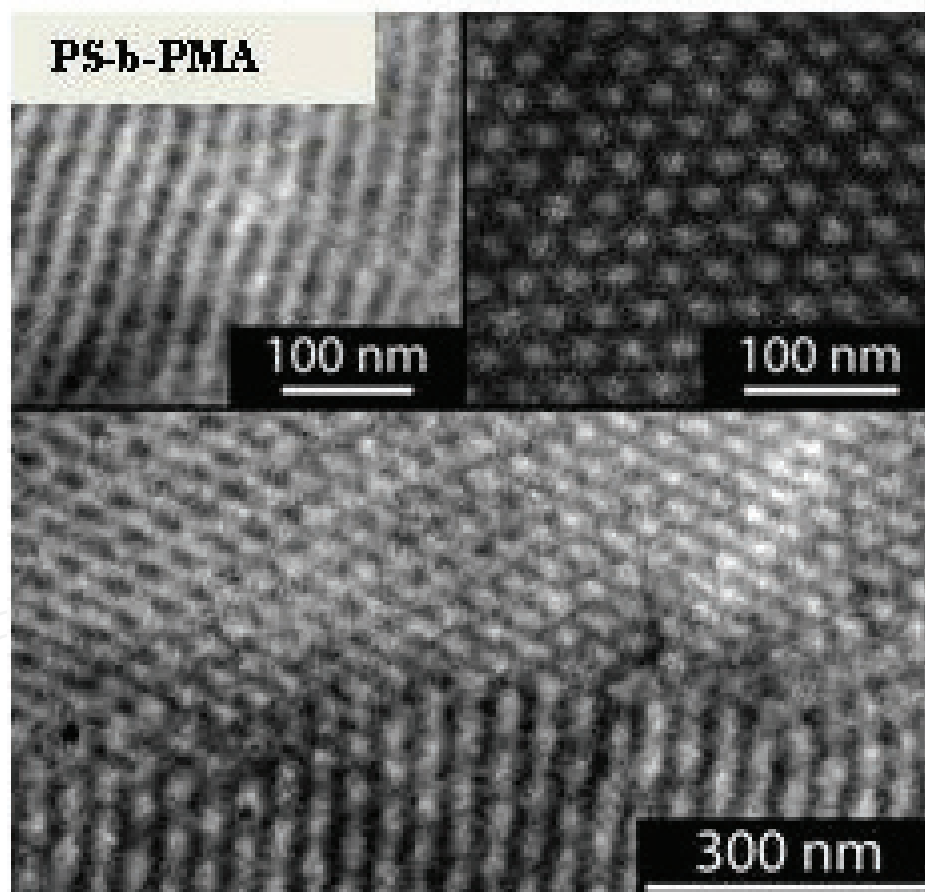

Figure 7. Bright field electron micrographs of PS-PMA samples after 72 h of thermal annealing at T = 120°C and staining with RuO_4 (PMA is dark domain). (PS-PMA)$_{NP}$: revealing HPL microstructure imaged at low magnification. The inset on the left depicts the PS-perforations within the PMA layers. The inset on the right shows a plane view revealing the hexagonal arrangement of the PS perforations. Reproduced with permission of [30]. Copyright 2008, American Chemical Society.

molecular weight distribution for the design of different microstructures with special topological properties for different potential applications.

For poly(styrene-*b*-isoprene) (PS-*b*-PI) copolymer thin films spin coated on mica [31], the formation of HPL morphology was found for a volume fraction of 38% for PS. The HPL layers were oriented parallel to the substrate and the perforations also presented the ABC-type stacking structure. They claimed that the transition from HPL to double gyroid (DG) always started from the substrate side, being the development of DG {121} plane parallel to the substrate. This confirmed the epitaxial conversion among HPL layers and DG {121} plane. For PS-*b*-PI copolymer with 70% of PS, some of the thermal annealed samples presented HPL morphology. Epitaxial relations of phase transitions between the lamellar, HPL, and G morphologies were investigated by SAXS and rheology [32]. In HPL to G transitions, six spot patterns of G phase were observed in two-dimensional SAXS pattern. On the other hand, in direct L to G transition without appearance of HPL phase, the polydomain patterns of G phase were observed. Direct L to G transition of blend may be suppressed by high-energy barrier of transition and mismatches in domain orientation between epitaxially related lattice planes.

For the same copolymer but with 65% of PS [33], it was concluded that order-order transitions between the L, HPL, and G phases proceeded through nucleation and growth. Maintaining the continuity of microphase-separated interfaces across the resulting grain boundaries involved considerable local distortion of both morphologies. The different geometrical characteristics of the phases and the imbalance in the spacings of epitaxially related lattice planes constituted the reason for that. There was an increase of the surface energy of the grains, which strongly restricted nucleation, avoiding direct L to gyroid transitions. The formation of the metastable HPL structure under such conditions reflected the ease with which the L to PL transition could occur compared to L to G one. Similar effects dominate the G to L transition. Very similar conclusions were obtained by the same authors [33] for poly((ethylene-co-propylene)-*b*-dimethylsiloxane) (PEP-*b*-PDMS) and poly (ethylene oxide-*b*-ethylethylene) (PEO-*b*-PPE) copolymers with 64 and 72% of PEP and PEO, respectively.

For PS-*b*-PPE copolymer [34], a thermo reversible mesophase transition between low-temperature HPL and high-temperature HPC was found. The transformation process was accompanied by a 6% change in the principal spacing, yet oriented specimens retained their macroscopic orientation through the transition. The cylinder to HPL transformation proceeded on a time scale of tens of minutes. At deep undercoolings, the transformation rate slowed due to a reduction in molecular mobility. By contrast, the HPL to C transformation occurred nearly 2 orders of magnitude more rapidly, a difference that reflected the nature of the dominant fluctuation modes for the two structures.

Finally, for a poly(ethylene oxide-*b*-butylene oxide) (PEO-*b*-PBO) copolymer with 71% vol PEO [35], it was also found that the transition from the L to the G phase proceeded via an intermediate PL structure. It was observed that the G phase developed from an oriented HPL phase precursor as an isotropic distribution of grains. This indicated that growth of this structure did not occur epitaxially on a macroscopic scale.

2.3. Hexagonally packed cylinders

Considered as one of the stable morphologies for asymmetric diblock copolymers, it has been found for many different copolymers [36–52] as a result of their composition or by different annealing processes. In that way, for amphiphilic poly(4-di(9,9-dihexylfluoren-2-yl) styrene)-*b*-poly(2-vinylpyridine) (PStFl2m-*b*-P2VPn) [36] copolymer thin films self-assembled into different nanostructures as a function of copolymer block ratio and film preparation process: random two phases, horizontal hexagonal P2VP cylinders, and hexagonally close packed (HCP) P2VP spheres. Authors found that the hexagonal cylinder and HCP morphologies were not similar to those found from block copolymers with similar compositions. Well-developed nanostructures were obtained for films annealed under CS_2 vapors and subsequent thermal annealing. Surprisingly, the solvent-annealed 50/50 copolymer films, either with or without subsequent thermal annealing, formed in-plane–oriented hexagonal P2VP cylindrical structure rather than L structure that was expected from an equivalent block composition. 75/25 copolymer films annealed under CS_2 vapors, independently of posterior thermal annealing, self-assembled into HCP P2VP structure. As a cylindrical structure was expected from copolymer composition, authors pointed out that it could be due to an annulation of the volume fraction rule. Those morphologies were found to make influences on the electrical memory performances of the polymers. In particular, the switching-ON voltage was influenced by the nanostructures and the film layer thickness as well as by the composition.

HPC morphology has also been observed for thin films of poly(styrene-*b*-tert-butyl acrylate) (PS-*b*-PtBA) with 60 wt% of PS, in contrast with the L morphology observed for the copolymer with 35 wt% of PS [37]. HPC morphology has also been observed for thin films of methyl methacrylate and polyhedral oligomeric silsesquioxane (POSS)-functionalized methacrylate (PMMA-*b*-PMAPOSS) diblock copolymer after solvent vapor annealing with CS_2 and Post-thermal annealing [42]. The exposure to solvent vapors generated perpendicularly oriented PMMA cylinders hexagonally packed in the PMAPOSS matrix. Even if before thermal annealing both blocks remained amorphous, the annealing process led to the crystallization of POSS moieties.

Nonequilibrium morphologies were also found for poly(styrene-*b*-4vinylpiridine) (PS-*b*-P4VP) (50/50) [43] by using a supramolecule. The copolymer assembled within the framework generated by the supramolecule, obtaining nonequilibrium morphologies that the sole copolymer could not reach. Perpendicularly oriented HPC domains formed first by the self-assembly of the supramolecules, based on symmetric (PS-*b*-P4VP) and 3-pentadecylphenol (PDP) linked to 4VP by hydrogen bonds, as it is shown in **Figure 8**. After selective removal of ~90% of the PDP and a brief solvent annealing in a chloroform atmosphere, symmetric PS-*b*-P4VP, containing a trace amount of PDP, self-assembled forming hexagonal microdomains oriented normal to the surface.

For PS-*b*-PI (32/68) copolymer thin films annealed at 182°C for 1 day and subsequently quenched to room temperature to freeze the structures, patterns of double gyroid (DG), HPC, and their coexisting phases were found [44]. A new epitaxial transition path among both
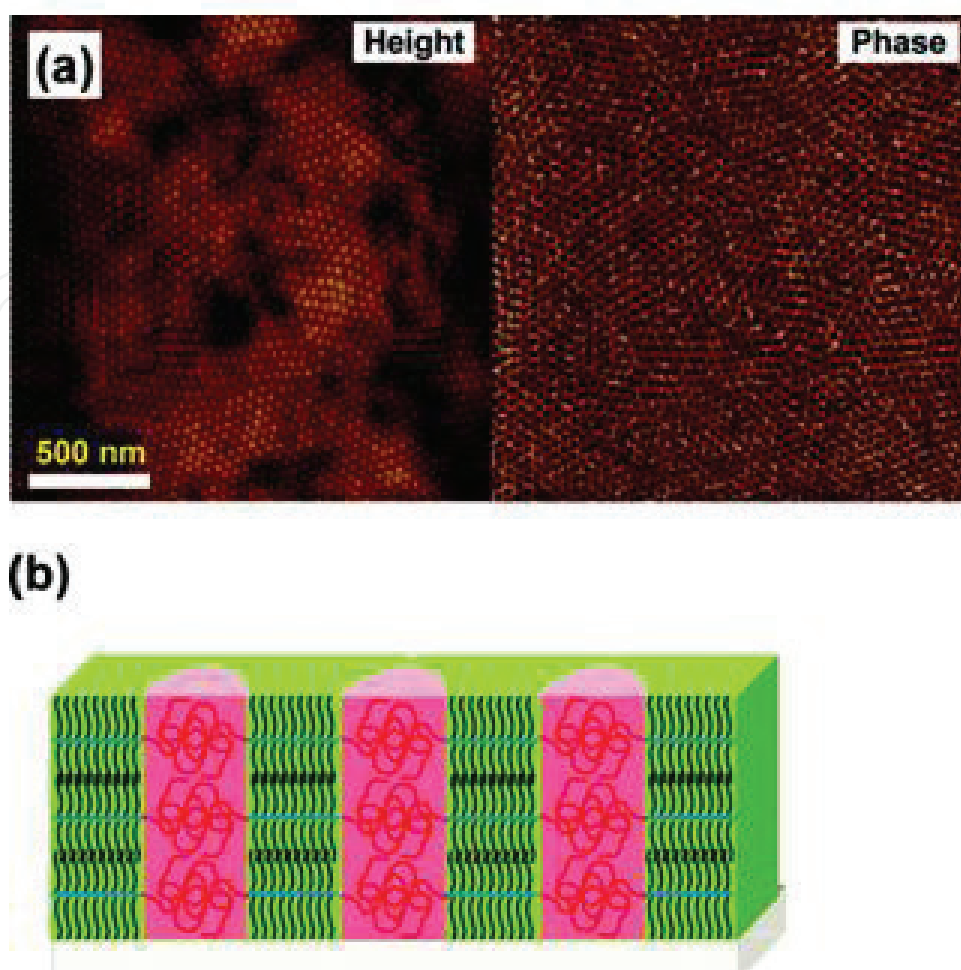
Figure 8. (a) SPM height and phase image of a PS(20,000)-*b*-P4VP(19,000)(PDP)$_1$ thin film, ~89 nm in thickness. The *z* scale is 15 nm for height and 30°for phase. (b) Schematic drawing of the cylinder-within-lamella hierarchical structure in thin films. Reproduced with permission of [43]. Copyright 2009, American Chemical Society.

nanostructures was found. This path seemed to have an advantage over the reported path in such a way that all the packed cylinders were converted from equivalent structures in DG while the previously reported path involved two different structures. In order to prepare nanoporous materials with periodic cylindrical holes, poly(butadiene-*b*-methylmethacrylate) (PB-*b*-PMMA) thin films that self-assembled into hexagonally packed PMMA cylinders in PB matrix were irradiated with γ-rays [45]. PMMA domains were removed by irradiation and succeeding solvent washing to form cylindrical holes within PB matrix, which was rigidified by radiation cross-linking: polymer nanoporous materials with periodic cylindrical holes were fabricated. For poly(ethylene oxide-*b*-styrene) (PEO-*b*-PS) copolymers with different block ratios, HPC [48] or inverse hexagonal cylinder (IHC) [47] morphologies have been found. For the 73/23 copolymer, IHC phase morphology was identified with PS HPC within the PEO matrix. Moreover, authors found that PEO blocks were tethered on the convex interfaces of the PS domains crystallizing outside of the cylinders. The orientation of PEO crystals changed with respect to the long cylinder axis due to the crystallization among PS

cylinders. Authors pointed out that it only depended on crystallization temperature. For 37/63 copolymer, on the other side, parallely-oriented HPC morphology was obtained. Order-order transition was observed by dynamic mechanical analysis to occur through a C to G transition.

For a poly(styrene-*b*-(ethylene-alt-propylene)) (PS-*b*-PEP) copolymer [34] a thermoreversible mesophase transition was found between low-temperature HPL and high-temperature HPC, which occurred in various tens of minutes. Even if it increased rapidly with undercooling, for strong undercoolings, the rate decreased probably because of a decrease in molecular mobility. On the contrary, the HPL to HPC transformation occurred much more rapidly. For asymmetric poly(ethylene oxide-*b*-isoprene) (PEO-*b*-PI) copolymer [51], crystallization of PEO block from oriented HPC was investigated. It was found that crystallization of PEO from a shear-oriented HPC led to crystalline lamellar planes parallel to the cylinders and a step increase in domain spacing. HPC morphology has also been found for PMMA-*b*-PVmTPA copolymer with a volume fraction of 0.73 for PMMA [29] and for poly(isoprene-*b*-methylmethacrylate) (PI-*b*-PMMA) copolymer [52] thin films annealed under acetone vapors, as it can be seen in **Figure 9**. Moreover, in the last case, the morphology was maintained after the addition of modified magnetic nanoparticles. Obtained nanocomposites presented magnetic properties.
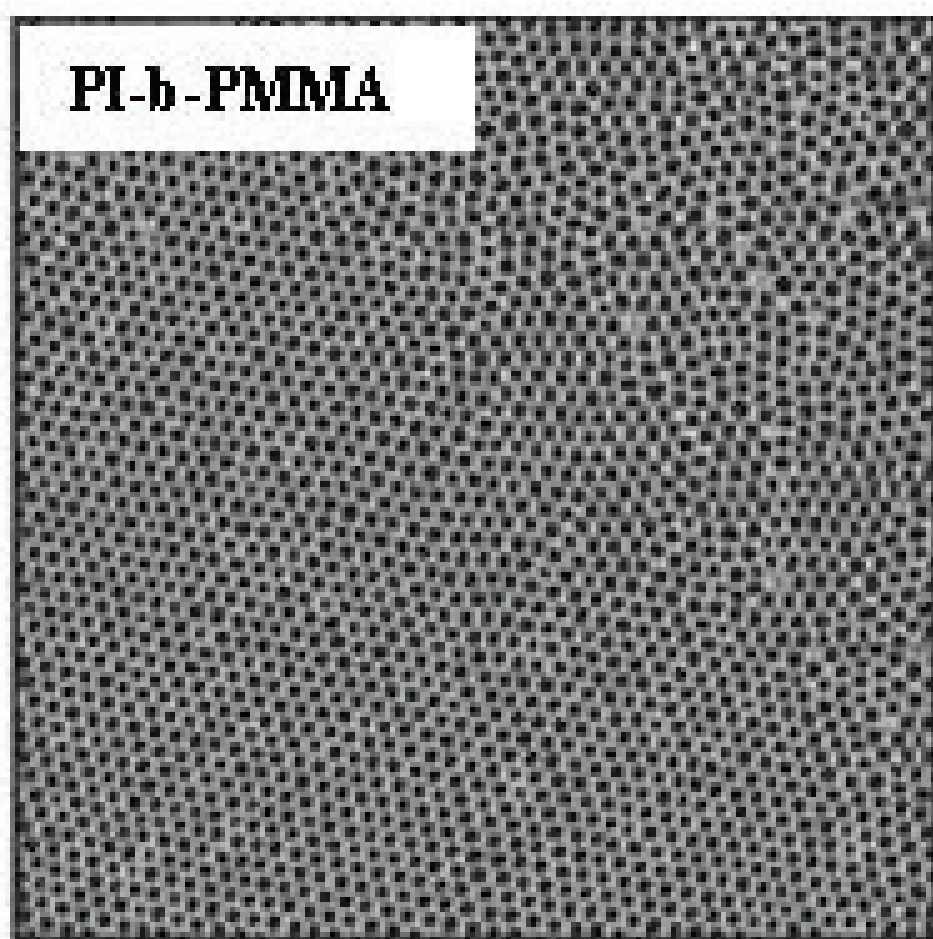

Figure 9. AFM phase images of PI-*b*-PMMA thin film annealed under acetone vapors solvent for 96 h. Reproduced with permission of [52]. Copyright 2016, Elsevier.

Liquid crystal (LC) block copolymers or copolymers containing a liquid crystal block has also been found to assemble into HPC structures [38, 39, 46, 49]. By working with a novel class of nanophase-separated and flexible double liquid crystalline EOBC-*b*-EOBCy diblock copolymers (EOBC and EOBCy monomers containing cyanobiphenyl mesogens) of different molecular weights but similar compositions [38], it was found that the diblock copolymer of higher molecular weight exhibited an exceptional order-order transition (OOT) from L to HPC upon nematic ordering. Obtained nanostructure type and size were determined by, besides the phase separation process, the flexibility of the polyether, and the mobility and order of the LC phases with different symmetries. Gopinadhan et al. [39] synthesized a novel liquid crystalline brush-like diblock copolymer, NBCB-*b*-NBPLA, using ring opening metathesis polymerization (ROMP), by sequential polymerization of functionalized norbornene (NB) monomers comprising cyanobiphenyl mesogens (CB) connected by 6 or 12 methylene units and poly(D,L-lactide) (PLA) chains of different lengths. They also used magnetic fields to direct the alignment of domains. By using copolymers with a NBPLA/NBCB ratio of 3:1, a morphology consisting on HPC of PLA was obtained. As the smectic mesophase presented diamagnetic anisotropy, the structure could be aligned by a magnetic field. HPC Domains of PLA minority block aligned parallely to the direction of an imposed magnetic field were obtained. By UV cross-linking and selective etching of PLLA, it was possible the fabrication of thermally switchable polymer films with aligned nanopores. Alignment of self-assembled hierarchical microstructure in LC diblock copolymers using high magnetic fields was also achieved for ferroelectric liquid crystalline diblock copolymer of poly(styrene-*b*-isoprene-LC), (PS-*b*-PILC), incorporating a biphenyl 3-nitro-4-alkoxybenzoate LC mesogenic group and a non-LC block. HPC microstructure was successfully accomplished by application of a magnetic field at elevated temperatures. LC block containing cylinders lied parallel to the field, allowing for the production of thin films of vertical or "standing" cylinders. HPC morphology was also found for a LC-type amphiphilic poly(ethyleneoxide-*b*-methacrylic acid) with azobenzene moieties, PEOm-*b*-PMA(Az)n, where *m* and *n* stand for the degrees of polymerization of the polymer part and the LC part, respectively. Polymer films were submitted to thermal and barometric effects under hydrostatic pressure. Nanoscale structures exhibited an HPC of PEO cylinders arrangement. The role of interfacial interactions between hydrophilic PEO and hydrophobic PMA(Az) including mesogen sequences in the side chains, at the isotropic transition, was analyzed and found to be of crucial importance.

Electric field–induced alignment of microphase-separated block copolymer domains has also been carried out for different copolymers such as PS-*b*-PVP, PS-*b*-PI or PS-*b*-PB [50]. Upon applying an electric field to the film, a morphology consisting on hexagonally packed cylinders was obtained for all copolymers. The microdomains were oriented inside the cylinders. Authors pointed out that obtained orientation depended on two competing factors: interfacial interactions and electric field. The control of the interfacial interactions allowed the obtention of parallely or perpendicularly oriented cylinders.

HPC has also been found for several copolymers synthesized for potential biological applications [40, 41]. In that way, uracil-functionalized poly(3-caprolactone)-*b*-(4-vinylbenzyl uracil)s (PCL-*b*-PVBU) were synthesized for their bioinspired assembly forming different

microstructures through nucleobase-induced supramolecular interactions [41]. The ordered morphologies of PCL-*b*-PVBU diblock copolymers changed from L to HPC or sphere morphologies with respect to the content of the hydrogen bond segment. Moreover, by hydrogen bonding between uracil and adenine groups, biocomplementary PCL-*b*-PVBU/9-hexadecyladenine (AC16), supramolecular complexes were formed. By using a nonstoichiometric PCL-*b*-PVBU/AC16 ratio, well-ordered L and HPC morphologies were obtained.

Finally, HPC has also been found for synthesized novel PEGylated polypeptide block copolymers of poly. The hierarchical self-assembly of their films led to the formation of L structures as a result of microphase separation of the diblock copolymers; HPC nanostructure featured α-helical conformations of PEGylated polypeptide segments, which were oriented perpendicularly to the director of the L structure formed by the diblock copolymers. These kinds of rod-coil block copolymers comprise an important class of nanomaterials because of their potential uses in biological and optoelectronic applications.

2.4. Gyroid morphology

The L and HPC morphologies cover a large range of compositions and molecular weights. In contrast, the gyroid (G) morphology corresponds to a narrow composition window at the weak segregation regime [2]. G morphology and transitions from lamellar or HPC morphologies to G ones have been found for different copolymers [32, 35, 44, 53–57], showing to have several potential applications.

For the production of devices as solar cells or special membranes, it results very interesting to obtain nanomaterials with connected pores. Thus, a way to prepare nanostructured porous materials would suppose a great advance for the design of such devices. As it seems to be difficult by common lithograpy, block copolymer lithography can be used as a "bottom up" approach, especially using DG structure. This morphology consists of two connected continuous networks of both blocks.

In that way, by using diblock copolymer-based PS-*b*-P4VP-(PDP) supramolecules that self-assemble into a bicontinuous gyroid morphology, metal nanofoams have been prepared [54]. G morphology consisted of PS network channels in a P4VP(PDP) matrix. After dissolving the PDP, the P4VP collapsed onto the PS struts and a bicontinuous gyroid interconnected template was obtained. The hydrophilic P4VP corona facilitated the penetration of water-based plating reagents into the porous template enabling a successful electroless metal deposition. Well-ordered inverse gyroid nickel foam was obtained after degrading the polymer by heating. Size and distribution of pores can be tuned by choosing the proper copolymer and PDP amount. As a candidate for the preparation of bicontinuous nanostructures for device fabrication, a poly(styrene-*b*-ferrocenylethylmethylsilane) (PS-*b*-PFEMS) diblock copolymer has been proposed [55]. The copolymer self-assembled into DG morphology. A block copolymer with a metal-containing block with iron and silicon in the main chain was selected due to its plasma etch resistance compared to the organic block, for further preparing nanoporous templates. Authors probed that DG morphology was the stable, equilibrium morphology of this copolymer.

The stability of G morphology at large segregation values was examined for poly(isoprene-*b*-ethylethylene) (PI-*b*-PEE) obtained by hydrogenation of PB block in PI-*b*-PB [57]. The large segregation values were achieved by the controlled and selective chemical modification of a precursor block copolymer, allowing χ to be varied over a large range at constant N. The complex bicontinuous gyroid structure was found to exist in a narrow window between the classical L and C morphologies. It was pointed out that the gyroid morphology remained even at segregation values (χN) much higher than those expected by theory and obtained experimentally. Authors performed annealing processes to the G phase, finding the same morphology and domain spacing. They obtained L and C structures by casting G samples with selective solvents. Samples were then thermally annealed, showing that G phase was again formed from cast phase. This seemed to indicate that G phase appeared as stable phase in the strong segregation regime.

A successful application of an ordered bicontinuous gyroid semiconducting network obtained from block copolymer template in a hybrid bulk heterojunction solar cell has been reported [56]. The freestanding G network was fabricated by electrochemical deposition into the 10 nm wide voided channels of a self-assembled, poly(4-fluorostyrene-*b*-lactide) (PFS-*b*-PLA) selectively degradable block copolymer film. Authors showed that the highly ordered pore structure was ideal for uniform infiltration of an organic hole transporting material, and solid-state dye-sensitized solar cells exhibited up to 1.7% power conversion efficiency. This patterning technique can be readily extended to other promising heterojunction systems consisting of a major step toward realizing the full potential of self-assembly in the next generation of device technologies. Schematic representation of the whole process can be seen in **Figure 10**.
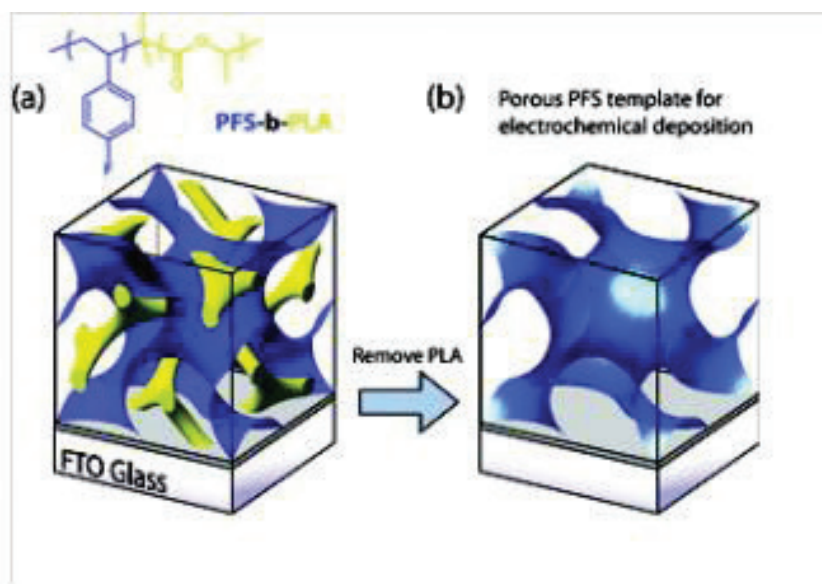

Figure 10. Schematic representation of the generation of porous PFS template for electrochemical deposition: a) preparation of PFS-*b*-PLA film onto FTO glass substrate and b) removal of PLA block. Reproduced with permission of [56]. Copyright 2009, American Chemical Society.

The epitaxial relations of phase transitions between the L, HPL and G morphologies were investigated for PS-*b*-PI (70/30) copolymer [32]. HPL to G transition was observed together with direct L to G one without appearance of HPL. Other authors also found the same transition for the same copolymer but with 38% of PS. In this case, films were prepared in mica substrate [31]. For thin films of PS-*b*-PI copolymer with 68% PI, however, a new epitaxial phase transition was found between DG and HPC structures [44]. The direction of phase transition, DG to HPC, was the main novelty of the work. A new epitaxial phase transition path from DG to HPC was described, which involved epitaxial relations between $\{121\}_{DG}$ and $\{10\}_{HPC}$ and between $\{111\}_{DG}$ and $\{11\}_{HPC}$. $\{220\}_{DG}$ became the grain boundary plane. The previously cited L to HPL to G transitions have also been found for films from other copolymers such as PEO-*b*-PBO [35], PEP-*b*-PDMS or PEO-*b*-PPE [33] prepared by melt-pressing. Their mechanisms have been well explained.

Finally, the ordered bicontinuous double diamond (OBDD) structure, that has long been believed to be an unstable ordered network nanostructure, relative to the ordered bicontinuous double gyroid (OBDG) structure for diblock copolymers, has been found for a copolymer composed of a stereoregular block, syndiotactic poly(propylene-*b*-styrene) (sPP-*b*-PS) [53]. The OBDD structure underwent a thermally reversible order-order transition (OOT) to OBDG upon heating. The thermodynamic stability of the OBDD structure was attributed to the ability of the configurationally regular sPP block to form helical segments, even above its melting point.

2.5. Spheres

Spherical morphology can consist mainly on body-centered cubic spheres (BCC), hexagonally close packed spheres (HP) or face-centered cubic spheres (FCC). Compared with the L and C nanostructures, the spheres of the BCC structure do not have anisotropy, and thus, the orientation of the BCC structure in thin films is in general less complicated than that of the HPC or L structures [58]. Morphology consisting on spheres has been found for several copolymers [36, 58–63]. Regarding to BCC morphology, it has been found for thin films of asymmetric poly(dimethylsiloxane-*b*-{2,5-bis[(4-butoxyphenyl)oxycarbonylstyrene}) (PDMS-*b*-PBPCS) (volume fraction of PDMS ranging from 10 to 23%) copolymer thermally annealed [58]. For all films, domains with a rectangular unit cell similar to the projection of the BCC lattice along the [110] direction were obtained. The orientation, parallel to the substrate, seemed to maximize the presence of PDMS at the substrate and at free interfaces. The surface layers of thin films were composed of both PDMS and PBPCS blocks. For copolymers with PDMS volume fractions of 10% and 13%, the neighboring [110]-oriented BCC domains matched well with each other, being the boundaries defect-free. For the copolymer with 23% of PDMS, PDMS spheres in the [110]-oriented BCC domains appeared overlapped with each other.

The mechanism and process of the thermally induced OOT of PS-*b*-PI diblock copolymer thin films from HPC morphology to BCC spheres have also been investigated [59]. Even if some studies dealing with the same kind of OOT have been reported [64, 65], authors investigated experimentally the epitaxial process by using a Bonse-Hart-type USAX apparatus [59], elucidating the mechanism and process of the thermally induced OOT.

BCC-sphere morphology has also been found for highly asymmetric poly(styrene-*b*-methacrylic acid) (PS-*b*-PMAA) copolymer [60]. The copolymer microphase-separated into spherical PMAA microdomains in a BCC arrangement in a PS matrix, in the strong segregation regime. It was found that the spherical microdomain morphology (with BCC symmetry) was favored over HPC morphology. BCC-type morphology has also been found for LC copolymers [61] such as poly(ethylene oxide)-*b*-(11-[4-(4-butylphenylazo)phenoxy]undecyl methacrylate)) (PEO-*b*-PMAAZ) one. For thermally annealed thin films, temperature-dependent phase transition behavior and the resulting morphologies were investigated. It formed a BCC structure of spherical PEO domains in the PMAAZ matrix, with both blocks in the amorphous state. The BCC structure was converted to HPC near 120°C, induced by the transformation of the isotropic phase of the PMAAZ matrix to the smectic A phase, composed of a laterally ordered structure of PMAAZ blocks with fully extended side groups. The resulting HPC structure was found to be very stable below 120°C, being retained as the smectic A phase of the PMAAZ matrix underwent further transitions to smectic C and to a smectic X phases.

Apart from BCC, other sphere symmetries have also been found in diblock copolymers [61–63]. For thin films of amphiphilic poly(4-di(9,9-dihexylfluoren-2-yl)styrene)-*b*-(2-vinylpyridine)) (PStFl$_{2m}$-*b*-P2VP$_n$) copolymer with a weight fraction of 73% for PStFl2 block, annealed under CS$_2$ vapors, a morphology consisting on hexagonally close packed (HCP) P2VP spheres was obtained rather than cylindrical structure which was expected from an asymmetric block composition [36], while for other compositions and annealing procedures, horizontal hexagonal P2VP cylinders or random two phases were found. The existence of FCC-packed spheres has also been probed for PEO-*b*-PB copolymer in the melt state [63]. The generation of FCC lattice took place by stacking together (111) planes in ABCABC sequence. It was noted that the FCC phase developed only by cooling from the disordered micellar phase.

Acknowledgements

Author details

Galder Kortaberria

Address all correspondence to: galder.cortaberria@ehu.eus

"Materials + Technologies" Group, University of the Basque Country (UPV/EHU), Donostia, Spain

References

[1] Bates FS, Fredrickson GH. Block copolymers-designer soft materials. Physics Today. 1999;**52**:32–38. DOI: 10.1063/1.882522

[2] Hamley IW. The Physics of Block Copolymers. Oxford University Press, Oxford, UK. 1999. p.432

[3] Leibler L. Theory of microphase separation in block copolymers. Macromolecules. 1980;**13**:1602–1617. DOI: 10.1021/ma60078a047

[4] Hadjichristidis N, Pispas S, Fluodas GA. Block copolymers: Synthetic strategies, physical properties, and applications. Wiley-interscience, Hoboken, USA. 2003

[5] Luo M, Epps TH. Directed block copolymer thin film self-assembly: Emerging trends in nanopattern fabrication. Macromolecules. 2013;**46**:7567–7579. DOI: 10.1021/ma401112

[6] Singh AN, Thake RD, More JC, Sharma PK, Agrawal JC. Block copolymer nanostructures and their applications: A review. Polymer-Plastics Technology and Engineering. 2015;**54**:1077–1095. DOI: 10.1080/03602559.2014.986811

[7] Yoo HG, Byun M, Jeong CK, Lee KJ. Performance enhancement of electronic and energy devices via block copolymer self-assembly. Advanced Materials. 2015;**27**:3982–3998. DOI: 10.1002/adma.201501592

[8] Balsara NP. Kinetics of phase transitions in block copolymers. Current Opinion in Solid State & Material Science. 1999;**4**:553–558. DOI: 10.1016/S1359-0286(00)00012-7

[9] Castelletto V, Hamley IW. Morphologies of block copolymer melts. Current Opinion in Solid State & Material Science. 2004;8:426–438. DOI: 10.1016/j.cossms.2005.06.001 DOI:10.1016/j.cossms.2005.06.001#doilink

[10] Matsen MW, Bates FS. Unifying weak- and strong-segregation block copolymer theories. Macromolecules. 1996;**29**:1091–1098

[11] Fasolka MJ, Mayes AM. Block copolymer thin films: Physics and applications. Annual Review of Material Research. 2001;31:323–355. DOI: 10.1146/annurev.matsci.31.1.323

[12] Nie T, Zhao Y, Xie Z, Wu C. Micellar formation of poly(caprolactone-*block*-ethylene oxide-*block*-caprolactone) and its enzymatic biodegradation in aqueous dispersion. Macromolecules. 2003;**36**:8825–8829. DOI: 10.1021/ma035131

[13] He CL, Sun JR, Deng MX, Chen XS, Jing XB. Study of the synthesis, crystallization, and morphology of poly(ethylene glycol)−poly(ε-caprolactone) diblock copolymers. Biomacromolecules. 2004;**5**:2042–2047. DOI: 10.1021/bm049720e

[14] Matsen MW, Schick M. Stable and unstable phases of a diblock copolymer melt. Physical Review Leters. 1994;**72**:2660–2663. DOI: 10.1103/PhysRevLett.72.2660

[15] Zhang J, Posselt D, Smilgies DF, Perlich J, Kyriakos K, Jaksch S, Papadakis CM. Lamellar diblock copolymer thin films during solvent vapor annealing studied by GISAXS: Different behavior of parallel and perpendicular lamellae. Macromolecules. 2014;**47**: 5711–5718. DOI: 10.1021/ma500633b

[16] Choi S, Kim E, Ahn H, Naidu S, Lee Y, Ryu DY, Hawker CJ, Russell TP. Lamellar microdomain orientation and phase transition of polystyrene-*b*-poly(methyl methacrylate) by controlled interfacial interactions. Soft Matter. 2012;**8**:3463–3469. DOI: 10.1039/ c2sm07297a

[17] Liang GD, Xu JT, Fao ZQ, Mai SM, Ryan AJ. Morphology of semicrystalline oxyethylene/oxybutylene block copolymer thin films on mica. Polymer. 2007;**48**:7201–7210. DOI: 10.1016/j.polymer.2007.09.049

[18] Barandiaran I, Cappelletti A, Strumia M, Eceiza A, Kortaberria G. Generation of nanocomposites based on (PMMA-PCL)-grafted Fe_2O_3 nanoparticles and PS-*b*-PCL block copolymer. European Polymer Journal. 2014;**58**:226–232. DOI: 10.1016/j.eurpolymj. 2014.06.022

[19] Busch P, Posselt D, Smilgies DM, Rheinlalnder B, Kremer F, Papadakis CM. Lamellar diblock copolymer thin films investigated by tapping mode atomic force microscopy: Molar mass dependence of surface ordering. Macromolecules. 2003;**36**:8717–8727. DOI: 10.1021/ma034375r

[20] Li Y, Kaito A. Highly oriented structure formed in a lamella-forming diblock copolymer with high molar mass. European Polymer Journal. 2006;**42**:1986–1993. DOI: 10.1016/j. eurpolymj.2006.04.007

[21] Pickett GT, Witten TA, Nagel SR. Equilibrium surface orientation of lamellae. Macromolecules. 1993;**26**:3194–3199. DOI: 10.1021/ma00064a033

[22] Park SM, Dong M, Rettner CT, Dandy DS, Wang Q, Kim HC. Bending of lamellar microdomains of block copolymers on non-selective surfaces. Macromolecules 2010;**43**:1665–1670. DOI: 10.1021/ma9020196

[23] Yamaguchi T, Yamaguchi H. Resist-pattern guided self-assembly of symmetric diblock copolymer. Journal of Photopolymer Science and Technology. 2006;**19**:385–388. DOI: 10.2494/photopolymer.19.385

[24] Kim SO, Solak HH, Stoykovich MP, Ferrier NJ, de Pablo JJ, Nealey PF. Epitaxial self-assembly of block copolymers on lithographically defined nanopatterned substrates. Nature. 2003;**424**:411–414. DOI: 10.1038/nature01775

[25] Kennemur JG, Yao L, Bates FS, Hillmyer MA. Sub-5 nm domains in ordered poly (cyclohexylethylene-b-methyl methacrylate) block copolymers for lithography. Macromolecules. 2014;**47**:1411–1418. DOI: 10.1021/ma4020164

[26] Bai WB, Hannon AF, Gotrik KW, Choi HK, Aissou K, Liontos G, Ntetsikas K, Alexander-Katz A, Avgeropoulos A, Ross CA. Thin film morphologies of bulk-gyroid polysty-

rene-block-polydimethylsiloxane under solvent vapor annealing. Macromolecules. 2014;**47**:6000–6008. DOI: 10.1021/ma501293n

[27] Heckmann M, Drossel B. Strong stretching theory for diblock copolymers in thin films. Journal of Chemical Physics. 2008;**129**:214903. DOI: 10.1063/1.3027437

[28] Nam TW, Jeong JW, Choi MJ, Baek KM, Kim JM, Hur YH, Kim YJ, Sik Jung YS. Single nanoparticle localization in the perforated lamellar phase of self-assembled block copolymer driven by entropy minimization. Macromolecules. 2015;**48**:7938–7944. DOI: 10.1021/acs.macromol.5b01931

[29] Mastroianni SE, Patterson JP, O'Reilly RK, Epps TH. Poly(methyl methacrylate-block-vinyl-mtriphenylamine): Synthesis by RAFT polymerization and self-assembly. Soft Matter. 2013;**9**:10146–10154. DOI: 10.1039/c3sm51806j

[30] Listak J, Jakubowski W, Mueller L, Plichta A, Matyjaszeski K, Bockstaller, MR. Effect of symmetry of molecular weight distribution in block copolymers on formation of "metastable" morphologies. Macromolecules. 2008;**41**:5919–5927. DOI: 10.1021/ma800816j

[31] Park HW, Im K, Chung B, Ree M, Chang T, Sawa K, Jinnai H. Direct observation of HPL and DG structure in PS-*b*-PI thin film by transmission electron microscopy. Macromolecules. 2007;**40**:2603–2605. DOI: 10.1021/ma062826c

[32] Ahn JH, Zin WC. Mechanism of morphological transition from lamellar/perforated layer to gyroid phases. Macromolecular Research. 2003;**11**:152–156. DOI: 1598–5032/06/152–05

[33] Hajduk DA, Ho RM, Hillmyer MA, Bates FS, Almdal K. Transition mechanisms for complex ordered phases in block copolymer melts. Journal of Physical Chemistry B. 1998;**102**:1356–1363. DOI: S1089–5647(97)02871-X

[34] Lai C, Loo YL, Register RA. Dynamics of a thermoreversible transition between cylindrical and hexagonally perforated lamellar mesophases. Macromolecules. 2005;**38**:7098–7104. DOI: 10.1021/ma050953n

[35] Hamley IW, Fairclough JPA,Ryan AJ, Mai SM,Booth C. Lamellar-to-gyroid transition in a poly(oxyethylene).poly(oxybutylene) diblock copolymer. Physical Chemistry Chemical Physics. 1999;**1**:2097–2101. DOI: 10.1039/A807847E

[36] Wi D, Ree BJ, Ahn B, Hsu JC, Kim J, Chen WC, Ree M. Structural details and digital memory performances of difluorene-containing diblock copolymers in nanoscale thin films. European Polymer Journal. 2016;**81**:582–597. DOI: 10.1016/j.eurpolymj.2015.12.011

[37] Pierre Escale P, Maud Save M, Billon L, Ruokolainenb J, Rubatat L. When block copolymer self-assembly in hierarchically ordered honeycomb films depicts the breath figure process. Soft Matter. 2016;**12**:790–797. DOI: 10.1039/c5sm01774b

[38] Wei W, Liu Y, Xiong H. Hierarchical nanostructures and self-assemblies in smectic-nematic liquid crystalline diblock copolymers. ACS Macroletters. 2014;**3**:892–895. DOI: 10.1021/mz500460j

[39] Gopinadhan M, Deshmukh P, Choo Y, Majewski PW, Bakajin O, Elimelech M, M. Kasi RM, Osuji CO. Thermally switchable aligned nanopores by magnetic-field directed self-assembly of block copolymers. Advanced Materials. 2014;**26**:5148–5154. DOI: 10.1002/adma.201401569

[40] Li PC, Lin YC, Chen M, Kuo SW. Self-assembled structures from PEGylated polypeptide block copolymers synthesized using a combination of ATRP, ROP, and click chemistry. Soft Matter. 2013;**9**:11257–11269. DOI: 10.1039/c3sm52061g

[41] Lin H, Cheng CC, Chuang WT, Chen JK, Jeng US, Ko FH, Chu CW, Huang CF, Chang FC. Bioinspired assembly of functional block-copolymer nanotemplates. Soft Matter. 2013;**9**:9608–9614. DOI: 10.1039/c3sm51870a

[42] Jin S, Hirai T, Ahn B, Rho Y, Kim KW, Kakimoto M, Gopalan P, Hayakawa T, Ree M. Synchrotron grazing incidence X-ray scattering study of the morphological structures in thin films of a polymethacrylate diblock copolymer bearing POSS moieties. Journal of Physical Chemistry B. 2010;**114**:8033–8042. DOI: 10.1021/jp1008785

[43] Tung SH, Xu T. Templated assembly of block copolymer toward non-equilibrium nanostructures in thin films. Macromolecules. 2009;**42**:5761–5765. DOI: 10.1021/ma900497j

[44] Park HW, Jung J, Chang T, Matsunaga K, Jinnai H. New epitaxial phase transition between DG and HEX in PS-b-PI. Journal of the American Chemical Society. 2009;**131**:46–47. DOI: 10.1021/ja808259m

[45] Sekine R, Sato N, Matsuyama T, Akasaka S, Hasegawa H. Radiation-induced fabrication of polymer nanoporous materials from microphase-separated structure of diblock copolymers as a template. Journal of Polymer Science: Part A: Polymer Chemistry. 2007;**45**:5916–5922

[46] Boyer SA, Grolier JPE, Yoshida H, Iyoda T. Effect of interface on thermodynamic behavior of liquid crystalline type amphiphilic diblock copolymers. Journal of Polymer Science: Part B: Polymer Physics. 2007;**45**:1354–1364. DOI: 10.1002/polb

[47] Huang P, Zheng JX, Leng S, Van Horn RM, Jeong KU, Guo Y, Quirk RP, Cheng SZD, Lotz B, Thomas EL, Hsiao BS. Poly(ethylene oxide) crystal orientation changes in an inverse hexagonal cylindrical phase morphology constructed by a poly(ethylene oxide)-block-polystyrene diblock copolymer. Macromolecules. 2007;**40**:526–534. DOI: 10.1021/ma061871h

[48] Mao H, Hillmyer MA. Macroscopic samples of polystyrene with ordered three-dimensional nanochannels. Soft Matter. 2006;**2**:57–59. DOI: 10.1039/b513958a

[49] Osuji C, Ferreira PJ, Mao G, Ober CK, Vander Sande JB, Thomas EL. Alignment of self-assembled hierarchical microstructure in liquid crystalline diblock copolymers using high magnetic fields. Macromolecules. 2004;**37**:9903–9908. DOI: 10.1021/ma0483064

[50] Xiang H, Lin Y, Russell TP. Electrically induced patterning in block copolymer films. Macromolecules 2004;**37**:5358–5363. DOI: 10.1021/ma049888s

[51] Hamley IW, Castelletto V, Floudas G, Schipper F. Templated crystallization from oriented gyroid and hexagonal melt phases in a diblock copolymer. Macromolecules. 2002;**35**:8839–8845. DOI: 10.1021/ma0207069

[52] Barandiaran I, Grana E, Katsiggianopoulos D, Avgeropoulos A, Kortaberria G. Nanocomposites based on nanostructured PI-b-PMMA and selectively placed PMMA-modified magnetic nanoparticles: Morphological and magnetic characterization. European Polymer Journal. 2016;**75**: 514–524. DOI:10.1016/j.eurpolymj.2016.01.005

[53] Chu CY, Jiang X, Jinnai H, Pei RY, Lin WF, Tsai JC, Chen HL. Real-space evidence of the equilibrium ordered bicontinuous double diamond structure of a diblock copolymer. Soft Matter. 2015;**11**:1871–1876. DOI: 10.1039/c4sm02608j

[54] Vukovic I, Punzhin S, Vukovic Z, Onck P, De Hosson JTM, Brinke GT, Loos K. Supramolecular route to well-ordered metal nanofoams. ACS Nano. 2011;**8**:6339–6348. DOI: 10.1021/nn201421y

[55] Gwyther J, Lotze G, Hamley I, Manners I. Double-gyroid morphology of a polystyrene-block-poly(ferrocenylethylmethylsilane) diblock copolymer: A route to ordered bicontinuous nanoscale architectures. Macromolecular Chemistry and Physics. 2011; **212**:198–202. DOI: 10.1002/macp.201000496

[56] Crossland EJW, Kamperman M Nedelcu M, Caterina Ducati C, Wiesner U, Smilgies DM, GES, Hillmyer MA, Ludwigs S, Steiner OU, Snaith HJ. A bicontinuous double gyroid hybrid solar cell. Nano Letters. 2009;**9**:2807–2812. DOI: 10.1021/nl803174p

[57] Davidock DA, Hillmyer MA, Lodge TP. Persistence of gyroid morphology at strong segregation in diblock copolymers. Macromolecules. 2003;**36**:4682–4685. DOI: 10.1021/ma034364y

[58] Shi LY, Li H, Lei WW, Ni W, Ran R, Pan Y, Fan XH, Shen Z. Extraordinary boundary morphologies of large-scale ordered domains of spheres in thin films of a narrowly dispersed diblock copolymer via thermodynamic control. Nanoscale. 2015;**7**:17756–17763. DOI: 10.1039/c5nr03837e

[59] Kimishima K, Saijo K, Koga T, Hashimoto T. Time-resolved high-resolution SAXS studies of OOT process and mechanism from hex-cylinder to BCC-sphere in a polystyrene-block-polyisoprene diblock copolymer. Macromolecules. 2013;**46**:9032–9044. DOI: 10.1021/ma401808p

[60] Ayoubi MA, Zhu K, Bo Nystrom B, Olsson U, Almdal K, Khokhlov AR, Piculell L. Morphological investigation of polydisperse asymmetric block copolymer systems of poly(styrene) and poly(methacrylic acid) in the strong segregation regime. Journal of Polymer Science, Part B: Polymer Physics. 2013;**51**:1657–1671. DOI: 10.1002/polb.23389

[61] Yoon J, Jung SY, Ahn B, Heo K, Jin S, Iyoda T, Yoshida H, Ree M. Order-order and order-disorder transitions in thin films of an amphiphilic liquid crystalline diblock copolymer. Journal of Physical Chemistry B. 2008;**112**:8486–8495. DOI: 10.1021/jp803664h

[62] Stein GE, Cochran EW, Katsov K, Fredrickson GH, Kramer EJ, Li X, Wang J. Symmetry breaking of in-plane order in confined copolymer mesophases. Physical Review Letters. 2007;**98**:158302. DOI: 10.1103/PhysRevLett.98.158302

[63] Huang YY, Hsu JY, Chen HL, Hashimoto T. Existence of fcc-packed spherical micelles in diblock copolymer melt. Macromolecules 2007;**40**:406–409. DOI: 10.1021/ma062149m

[64] Matsen MW. Cylinder-sphere epitaxial transitions in block copolymer melts. Journal of Chemical Physics. 2001;**114**:8165–8173. DOI: 10.1063/1.1365085

[65] Kimishima K, Koga T, Hashimoto T. Order−order phase transition between spherical and cylindrical microdomain structures of block copolymer. I. Mechanism of the transition. Macromolecules. 2000;**33**:968–977. DOI: 10.1021/ma991470k